IEEE Access
Multidisciplinary | Rapid Review | Open Access Journal

Received 15 October 2023, accepted 4 November 2023, date of publication 8 November 2023,
date of current version 13 November 2023.

Digital Object Identifier 10.1109/ACCESS.2023.3330965

RESEARCH ARTICLE

Dual-Polarization Hermite-Gaussian-Based NFDM Transmission System

MUYIWA BALOGUN[1], STANISLAV DEREVYANKO[2], AND LIAM BARRY[1], (Senior Member, IEEE)
[1]School of Electronic Engineering, Dublin City University, Dublin 9, D09 V209 Ireland
[2]School of Electrical and Computer Engineering, Ben Gurion University of the Negev, Beer Sheva 84105, Israel

Corresponding author: Muyiwa Balogun (balogun.muyiwablessing@dcu.ie)

This work was supported in part by the Science Foundation Ireland under Grant 12/*RC*/2276_*P*2, and in part by the European Union's Horizon 2020 Research and Innovation Program under the Marie Skłodowska-Curie under Grant 847652.

ABSTRACT The nonlinear frequency division multiplexing (NFDM) transmission scheme continues to attract high interests in optical communications due to its robustness against nonlinearity and dispersion. The use of Hermite Gaussian (HG) wave-carriers has been proposed and has been shown to out-perform conventional methods used by state-of-the-art single polarization NFDM systems due to their excellent time-bandwidth-product (TBP) efficiency. In this work, employing the Manakov model, we investigate and demonstrate, for the first time, a high-capacity dual polarization NFDM (DP-NFDM) transmission system based on HG wave-carriers, enhanced by a single parameter equalizer. We report here, a record high spectral efficiency of 12 bits/s/Hz for dual-polarization HG-based DP-NFDM systems.

INDEX TERMS Optical communications, nonlinear frequency division multiplexing, NFDM, Hermite-Gaussian, NFT, dual polarization.

I. INTRODUCTION

Currently, optical fiber communication systems are fast approaching their capacity threshold [1], [2], [3]. The recently proposed nonlinear frequency division multiplexing (NFDM) scheme is seen as a very potent solution to the problem imposed by Kerr nonlinearity, that has limited the capacity of existing optical communications systems [4], [5]. The key idea of the NFDM scheme is that after performing a special nonlinear Fourier transform (NFT) on the signal, the evolution of the resulting *nonlinear spectrum* during signal propagation is trivial and can be easily compensated. Therefore, it is possible to encode the data directly on the nonlinear spectrum, obtain a waveform at the transmitter by means of the inverse nonlinear Fourier transform (INFT) operation, launch the signal into the optical channel and ultimately, recover the sent data by means of forward NFT and propagation compensation [6]. The NFDM scheme, which has been shown to be capable of eliminating issues such as the nonlinear cross-talk, however, has its own drawbacks [7], [8]. One of the main drawbacks is the fact that NFDM systems by design are limited to the burst mode, which leads to poor time-bandwidth-product (TBP) [9], thereby limiting the achievable information rate (AIR) of the system [5].

Recently, some of us proposed the use of Hermite-Gaussian (HG) wave-carriers [10], [11], as alternatives to the commonly used sinc-based carriers. The HG wave-carriers are known to possess low TBP and excellent localization properties, both in the time and frequency domains [12]. These properties are also carried forward to the nonlinear domain, which enabled us to achieve up to 4.45 bits/s/Hz spectral efficiency (SE) for a single polarization 32-QAM system at baud rates above 20 Gbaud [11]. However, since previous works on HG-based NFDM have focused only on the implementation of single polarization systems, it stands to reason to investigate the possibility of doubling the capacity by implementing a dual polarization (DP) NFDM system based on HG wave-carriers.

Therefore, this work seeks to investigate and demonstrate the possibility of achieving dual polarization for HG-based NFDM systems, employing the Manakov model, while

The associate editor coordinating the review of this manuscript and approving it for publication was Chao Zuo.

exploring high modulation formats. The main performance degrading factors in the NFDM transmission are not chromatic dispersion and Kerr nonlinearity but rather inline amplifier spontaneous emission (ASE) and the so-called processing noise. The latter is a deterministic spectral distortion stemming from insufficient sampling, burst clipping and other deterministic model imperfections [13].

To mitigate it, we implement a practical mean square error (MSE) equalization technique, based on a single complex parameter equalizing the constellation distortion and rotations. This has allowed us to achieve a high SE of 12 bits/s/Hz for both polarizations, which constitutes a record, to the best of our knowledge, for DP-NFDM-based schemes. When normalized per polarization, these results exceed previous NFDM SE record of 5.5 bits/s/Hz for *single polarization* reported recently in [14] for traditional sinc-based b-modulation, where the authors employed an off-line pre-training of a linear minimum mean-squared error estimator at the receiver.

The current submission is the extension of the work presented in [15]. We have added the comparison with a conventional system operating at similar baudrate. Also, we have included the study of the bandwidth dependence on the linear power, as well as the influence of neighboring bursts and constellation cardinality on the overall system performance.

II. THE HG-BASED DP-NFDM TRANSMISSION

In this work, we consider a dual-polarization optical fiber channel, which is described by the path-averaged Manakov equation [16]

$$\frac{\partial \overrightarrow{Q}}{\partial z} + j\frac{\beta_2}{2}\frac{\partial^2 \overrightarrow{Q}}{\partial t^2} - j\frac{8}{9}\gamma' \| \overrightarrow{Q} \|^2 \overrightarrow{Q} = \overrightarrow{n}, \tag{1}$$

where $\gamma' = \gamma(1 - e^{-\alpha L_a})/(\alpha L_a)$, $j = \sqrt{-1}$ and $\overrightarrow{Q}(t, z)$ is a 2-component complex envelope $\overrightarrow{Q}(t, z) = [Q_1(t, z),\ Q_2(t, z)]^T$, which is a function of time t and distance z along the optical fiber link. Also, γ, α, and β_2 denote the Kerr nonlinearity, fiber loss coefficient, and chromatic dispersion respectively, with span of length L_a. In NFT-based transmission schemes, the model is usually presented in the normalized soliton units, when the time is normalized to a characteristic pulse duration T_n, $T = t/T_n$, and z is normalized by a dispersion length, $L_D = T_n^2/|\beta_2|$, while the envelope also is normalized to a nonlinear power $q = Q(8\gamma' L_D/9)^{1/2}$. The effects of the amplifier spontaneous emission noise, are given by the $\overrightarrow{n}(z, t)$ term, which we assume as a complex white Gaussian process. This distributed noise model is exact in the case of ideal distributed Raman amplification [1] (where one must put $\gamma' = \gamma$) but also applies to the path-averaged description of a lumped erbium-doped fiber amplification scheme, after the appropriate re-normalization of the nonlinear coefficient [17]. In conventional NFDM, the data are encoded in the nonlinear frequency spectrum and modulated directly on the so-called b-coefficient at the transmitter as in [18] and [19], where sinc-based carriers were used. This is the b-modulation version of the NFDM, which has by now replaced the original suggestion in [4] and [5].

The general scheme of the NFDM transmission that follows is given in Fig.1. Here, we use the same scheme but for dual polarization scenario, using the (I)NFT algorithm described in [20]. The algorithm relies on Ablowitz-Ladik and discrete layer peeling (DLP) methods and represents a generalization of the similar approach for the scalar case. Additionally, we apply the HG wave-carriers as was previously done in [11] for a single polarization. We use an exponential squeezing mapping as in [18] to ensure that the vector b-coefficient obeys the necessary constraint $\|\vec{b}\| \leq 1$ (see e.g. [20], [21]). Thus, for the initial b-coefficient at the transmitter, we obtain the following expression:

$$\begin{aligned}
\overrightarrow{b}(0, \xi) &= \frac{\left[1 - \exp\left(-\|\overrightarrow{u}(0, \xi)\|^2\right)\right]^{1/2}}{\|\overrightarrow{u}(0, \xi)\|}\overrightarrow{u}(0, \xi), \\
u_i(0, \xi) &= \sqrt{S}\sum_{n=0}^{N-1} c_{n,i} f_n(\xi), \\
f_n(\xi) &= \frac{H_n(\xi)}{\sqrt{2^n\, n!\, \sqrt{\pi}}} e^{-\xi^2/2},
\end{aligned} \tag{2}$$

where $i = 1, 2$ labels polarization components, ξ denotes the "nonlinear frequency", $c_{n,i}$ are a set of N transmitted symbols in each polarization, $S > 0$ is the power scaling factor and $f_n(\xi)$ is the Hermite-Gaussian function of order n, with

$$H_n(\xi) = (-1)^n e^{\xi^2} \frac{d^n}{d\xi^n} e^{-\xi^2}. \tag{3}$$

As mentioned earlier, the main benefit of using the HG subcarriers is that they offer low TBP as well as higher spectral efficiency as they possess excellent localization properties both in the linear and nonlinear Fourier domain [10], [12].

The initial spectrum as described in (2) is then pre-compensated, transformed in the time domain and propagated through the fiber channel - see Fig. 1. At the receiver, the orthogonality of the HG carriers, like the commonly used sinc-based carriers, allows for a simple demodulation process, where the coherently detected received signal is forward NFT-transformed, and projected on different sub-carriers for symbol recovery.

In this work, we use the Q-factor (defined via bit error rate as $Q = 20\log(\sqrt{2}\mathrm{erfc}^{-1}(2\,BER))$), as well as the spectral efficiency as the figures of merit. The spectral efficiency (SE) is obtained via the achievable information rate (AIR) [22]. The latter represents the lower bound for the channel mutual information (and hence channel capacity) when the receiver is assumed to be optimized not for the unknown channel law but for an auxiliary (mismatched) channel, which we have assumed here as a complex Gaussian. Assuming symbol-wise detection and that the symbols are sampled uniformly from a constellation χ_M of cardinality M, the AIR per polarization

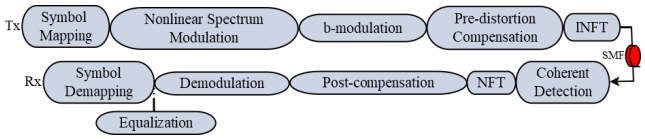

FIGURE 1. A simple NFDM schematic diagram.

is obtained as

$$\begin{aligned} AIR &= \mathbb{E}\big[\log_2 CN\{Y_k|X_k, \sigma^2(X_k), \tilde{\sigma}^2(X_k)\} - \log_2 P(Y_k)\big], \\ P(Y_k) &= \frac{1}{M}\sum_{x\in\chi_M} CN\{Y_k|x, \sigma^2(x), \tilde{\sigma}^2(x)\}, \\ \sigma^2(x) &= \mathbb{E}\Big[|Y(x)-x|^2\Big], \quad x \in \chi_M \\ \tilde{\sigma}^2(x) &= \mathbb{E}\Big[(Y(x)-x)^2\Big], \quad x \in \chi_M \end{aligned} \tag{4}$$

where $CN\{Y|X, \sigma^2, \tilde{\sigma}^2\}$ represents a uni-variate complex Gaussian distribution function with mean X, covariance σ^2 and pseudo-covariance $\tilde{\sigma}^2$, while the averaging is carried out over multiple generated input-output symbol pairs denoted as $\{X_k, Y_k\}$ [18], [19]. After obtaining the AIR, the SE can be calculated as

$$SE = \frac{2\,N\,AIR}{T_b\,W_d}\ \text{[bits/s/Hz]}. \tag{5}$$

where the factor 2 accounts for 2 polarizations, T_b represents the NFDM burst width and W_d is the *linear* bandwidth, which in this case is defined as the spectral window containing 99% of the burst energy (other threshold values are discussed in Section IV). Generally, NFDM systems are implemented using burst mode transmission as most NFT-based schemes rely on time localized pulse decaying to zero [5] (as in fact many other analog and digital communication systems). Hence, information is transmitted in a burst of width T_b, which includes, apart from the information sequence, a guard band usually determined by the dispersion-induced spreading of the pulse. If we denote by T_d the 99% energy window of the burst, which is the INFT of the initial spectrum (2), then it is common to express the SE penalty as $\eta = T_b/T_d$ [11], [18], [19]. The spectral efficiency as described in (5) can then be rewritten as $SE = 2\,N\,AIR/(TBP \times \eta)$, where $TBP = W_d \times T_d$ represents the time bandwidth product.

III. THE SINGLE PARAMETER EQUALIZER

The ultimate goal of NFDM is to seek ways by which the spectral efficiency of the optical transmission system can be optimized. One way to achieve this is by ensuring shorter burst duration by using the SE penalty $\eta < 1$ [11]. Achieving this, however, leads to pulse clipping and signal degradation [18], [19]. The resulting nonlinear spectral distortion is a significant part of the processing noise [13], which at high launch powers dominates over the ASE noise contribution [11], [19].

In order to address the degradation in signal quality and the overall performance, we implement a simple MSE equalization based on a single complex parameter K. This is achieved in a practical way by selecting a small amount of pilot symbols for training. In this work, we used the first 10 bursts such that if each contains N subcarriers in each polarization, then $N_p = 2 \times 10 \times N$ pairs of input-output constellation points are used. The simple equalizer, which tries to minimize the mean square error of the received symbols can be described as

$$K^* = arg\ min \frac{1}{N_p}\sum_{n=0}^{N_p-1} |Kc_n^{out} - c_n^{in}|^2, \tag{6}$$

where $[c_n^{in}]_{n=0}^{N_p-1}$ and $[c_n^{out}]_{n=0}^{N_p-1}$ are the sequences of sent pilots and the corresponding received symbols in two polarizations respectively. The loss function can be easily minimized analytically to obtain

$$K^* = \frac{\sum_{n=0}^{N_p-1} \bar{c}_n^{out}\, c_n^{in}}{\sum_{n=0}^{N_p-1} |c_n^{out}|^2}, \tag{7}$$

where the over-bar stands for the complex conjugate. The obtained correction factor is then multiplied by the received sample for the remaining runs and the Q-factor and SE are calculated for those corrected values.

TABLE 1. The parameters of the fiber link.

Parameter	Value
Group velocity dispersion, β_2	-21 ps^2/km
The nonlinear coefficient, γ	1.27 W^{-1} km^{-1}
Fiber loss, α	0.2 dB km^{-1}
Time normalization value, T_n	50 ps
Number of spans	12
Total propagation length	800 km
The number of the nonlinear subcarriers, N	32, 64
Constellation	32, 64, 128, 256-QAM
EDFA noise figure	5 dB

IV. SIMULATION RESULTS

In this section, we discuss the overall performance of the implemented HG-based DP-NFDM transmission system, employing b-modulation with the simple equalization discussed above. We considered high order QAM formats using 32-QAM, 64-QAM, 128-QAM and 256-QAM. The system parameters of the optical fiber link used are given in Table 1.

In Fig. 2, the graph shows a plot of the Q-factor (obtained by direct error counting) against the launch power for various values of the burst width (controlled by the parameter η), with and without equalization, for a 32-QAM system with $N = 32$ HG subcarriers in each polarization. The corresponding typical baudrate was $N/T_b = 22$ Gbaud per polarization corresponding to the burst width $T_b = 7.4$ ns. The plot shows the advantage of the equalizer, offering a gain of up to $1dB$ for various values of η. The gain from the implemented equalizer enabled us to achieve a more aggressive burst clipping, while ensuring an improved signal quality, such that even at $\eta = 0.92$, we are able to obtain a performance close to the 7% HD-FEC threshold set as the benchmark for tolerable quality of transmission. The implication of the

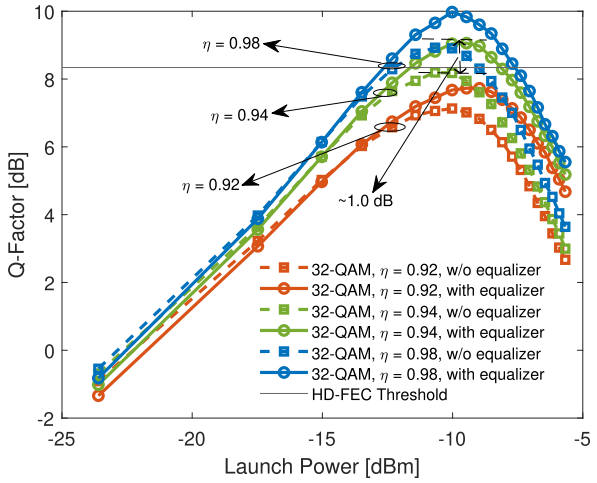

FIGURE 2. The Q-factor of the HG-based DP-NFDM transmission for a 32-QAM system.

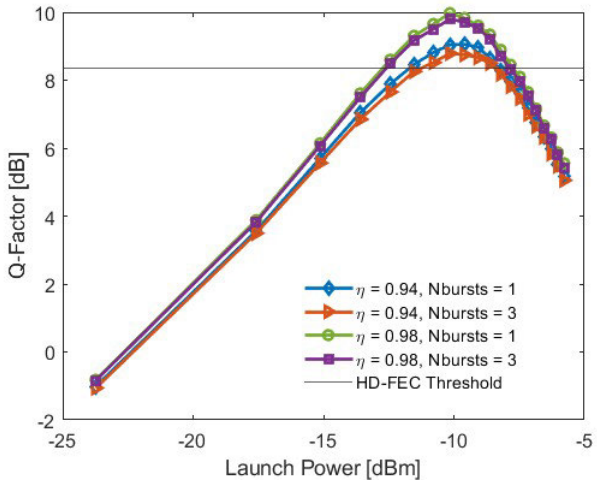

FIGURE 3. Q-factor graph with different number of bursts.

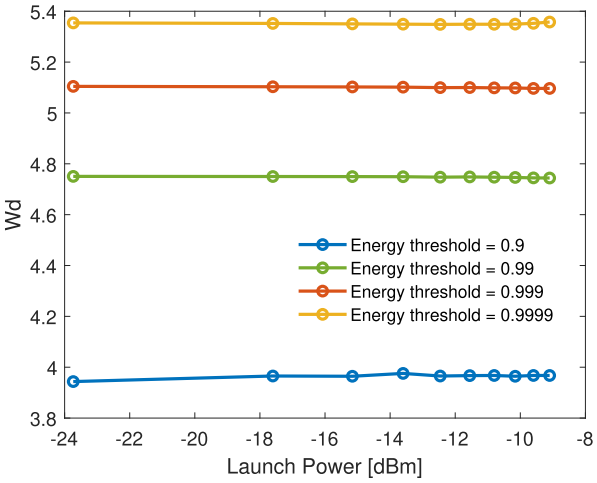

FIGURE 4. Defined linear bandwidth (GHz) versus Launch power graph for a 32-QAM system.

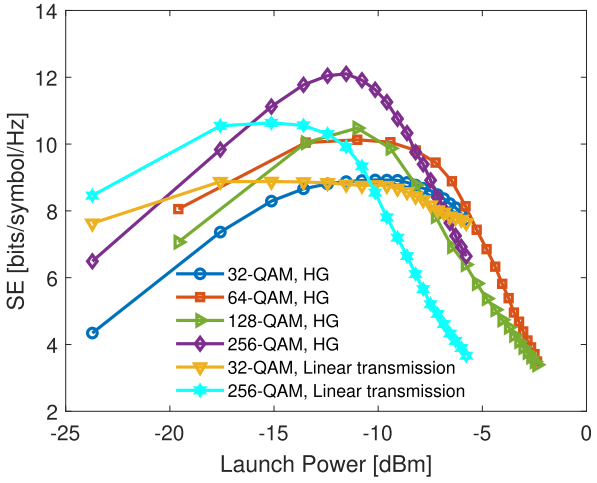

FIGURE 5. The spectral efficiency of the HG-based DP-NFDM and a linear benchmark system for different orders of modulation format.

aggressive burst clipping, which the equalizer has afforded us, is that we are able to obtain improved performance for reduced values of η for the implemented dual polarization transmission. Achieving this is very important, since being able to keep the burst duration smaller than the width of the pulse, as much as possible is key to achieving high SE.

For the channel simulation in the above results, we used a standard split-step Fourier method. While in Fig.2, we implemented a single burst during our simulations, we have also put into consideration the effects of inter-burst interaction by fixing the computational window equal to the (clipped) burst width T_b and refraining from using absorbing boundary condition. Therefore, the tails of the burst appearing during the dispersion broadening are effectively back-reflected to the computational window, thus, leading to the burst self-interaction. To check that this scheme is accurate, we have also performed simulations with different number of bursts. The results are shown in Fig. 3, where we have shown the plot of the Q-factor for different number of bursts and SE penalty parameter. One can see that the influence of the neighbouring bursts on the central burst of interest is accurately modeled by a single burst model with periodic BC.

In our publication we use 99% energy threshold for defining a *linear bandwidth* W_d following our previous publications [10], [11]. This may seem like an arbitrary value and other researchers may consider different criteria. Therefore, in order to elucidate the matter, in Fig. 4, we provide the power dependence of the linear bandwidth for a 32-QAM system for different values of the energy threshold. One can see that raising the threshold from 99% to 99.99% (as used for example in [9]), results in the increase of the linear bandwidth W_d from 4.75 GHz to 5.3 GHz (i.e. SE degradation of only 12%). Also note that the power dependence in the interval shown is negligible (although the bandwidth does go up at higher values of input power >-5 dBm when the performance is degraded by the processing noise [13], [19]). This graph can also be used by adjusting the SE results for different bandwidth definitions.

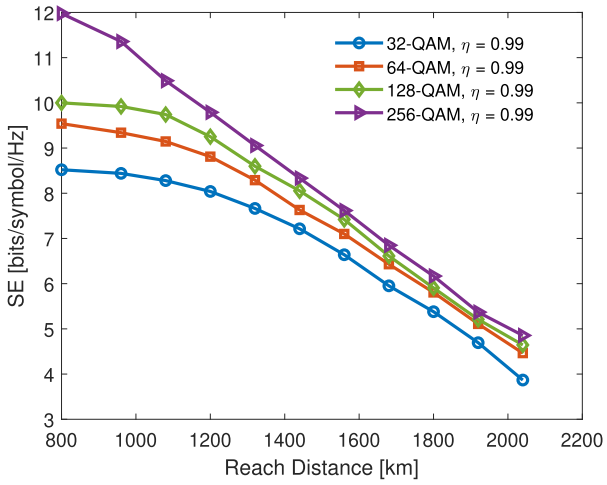

FIGURE 6. The spectral efficiency of the HG-based DP-NFDM versus the reach distance.

Next we study the effect of the modulation constellation cardinality on the SE. The results are shown in Fig. 5. In order to give a better perspective to this work, we added the performance of a 32/256-QAM conventional linear transmission systems as a benchmark. For the linear benchmark systems, we used a single channel root raised cosine, with a roll-off factor of 0.1. The parameters of the linear system were chosen to match exactly the baudrates of its NFDM HG counterpart (22 Gbaud for 32 QAM and 82 Gbaud for 256 QAM respectively). Linear dispersion compensation was also performed at the receiver for the benchmark system. We did not use full digital back-propagation as its performance depends on the number of steps per span as an additional parameter and it was not our goal to provide an extensive comparison with the conventional systems (see early publication on NFDM [6], [17] for such a comparison).

From the results of Fig. 5, one can see the advantage of the implemented equalizer in combination with dual polarization Hermite-Gauss NFDM scheme. For example we were able to achieve SE ranging from 9 bits/s/Hz for two polarizations for the 32-QAM system, to a record high 12 bits/s/Hz for the 256-QAM system considered. Of course, one must keep in mind that our definition of SE (5) depends explicitly on the spectral energy threshold used in the definition of the linear bandwidth (see Fig.4) and here we use the 99% value. One can also see that the NFDM outperforms the conventional benchmark counterpart at higher constellation cardinalities.

Finally, the plot of the spectral efficiency versus the reach distance is shown in Fig. 6. The performance is expectedly degraded with the distance owing to the accumulating ASE noise - signal interaction in the nonlinear domain [19], [23]. However, in this work, the implemented HG-based DP-NFDM, aided by the equalizer, shows good performance and efficiency over long distance. In [18], where sinc-based carriers were used, a maximum spectral efficiency of 7.2 bits/s/Hz was reported for a 960 km long-haul dual polarization NFDM system. Here, this spectral efficiency value was achieved around 1500 km, which is significantly higher than the reach distance reported previously in [18]. This shows the viability of the implemented system as it offers a desirable signal quality and spectral efficiency over long reach distance.

V. CONCLUSION

In this paper, for the first time, we have implemented a high modulation format dual polarization NFDM based on HG wave-carriers. We demonstrated that the implemented transmission system can be further enhanced by a practical and simple equalizer, based on a single value parameter. Aside the signal degradation due to residual phase rotation, pulse clipping, undersampling (i.e. the processing noise), the system experiences traditional random distortion due to ASE noise accumulation. However, by using the low time-bandwidth product of the HG wave-carriers, together with a simple low-complexity equalizer, we were able to achieve a record high SE value (for NFDM) of up to 12 bits/s/Hz total for two polarizations. Furthermore, we demonstrated that the reach distance can be significantly improved, while maintaining good signal quality and achieving acceptable SE values. This work further consolidates the high potential of HG wave-carriers as very viable enhancement of the currently used NFT-based schemes.

REFERENCES

[1] R.-J. Essiambre, G. Kramer, P. J. Winzer, G. J. Foschini, and B. Goebel, "Capacity limits of optical fiber networks," *J. Lightw. Technol.*, vol. 28, no. 4, pp. 662–701, Feb. 2010.
[2] A. D. Ellis, M. E. McCarthy, M. A. Z. Al Khateeb, M. Sorokina, and N. J. Doran, "Performance limits in optical communications due to fiber nonlinearity," *Adv. Opt. Photon.*, vol. 9, no. 3, pp. 429–503, Sep. 2017.
[3] P. Bayvel, R. Maher, T. Xu, G. Liga, N. A. Shevchenko, D. Lavery, A. Alvarado, and R. Killey, "Maximizing the optical network capacity," *Philos. Trans. Roy. Soc. A, Math., Phys. Eng. Sci.*, vol. 374, Mar. 2016, Art. no. 20140440.
[4] M. Yousefi and F. Kschischang, "Information transmission using the nonlinear Fourier transform, Part I: Mathematical tools," *IEEE Trans. Inf. Theory*, vol. 60, no. 7, pp. 4312–4328, Jul. 2014.
[5] S. K. Turitsyn, J. E. Prilepsky, S. T. Le, S. Wahls, L. L. Frumin, M. Kamalian, and S. A. Derevyanko, "Nonlinear Fourier transform for optical data processing and transmission: Advances and perspectives," *Optica*, vol. 4, no. 3, p. 307, 2017.
[6] J. E. Prilepsky, S. A. Derevyanko, K. J. Blow, I. Gabitov, and S. K. Turitsyn, "Nonlinear inverse synthesis and eigenvalue division multiplexing in optical fiber channels," *Phys. Rev. Lett.*, vol. 113, no. 1, Jul. 2014, Art. no. 013901.
[7] S. Civelli, E. Forestieri, and M. Secondini, "Why noise and dispersion may seriously hamper nonlinear frequency-division multiplexing," *IEEE Photon. Technol. Lett.*, vol. 29, no. 16, pp. 1332–1335, Aug. 15, 2017.
[8] S. Civelli, E. Forestieri, and M. Secondini, "Mitigating the impact of noise on nonlinear frequency division multiplexing," *Appl. Sci.*, vol. 10, no. 24, p. 9099, Dec. 2020. [Online]. Available: https://www.mdpi.com/2076-3417/10/24/9099
[9] A. Span, V. Aref, H. Bülow, and S. T. Brink, "Time-bandwidth product perspective for nonlinear Fourier transform-based multi-eigenvalue soliton transmission," *IEEE Trans. Commun.*, vol. 67, no. 8, pp. 5544–5557, Aug. 2019.
[10] M. Balogun and S. Derevyanko, "Hermite-Gaussian nonlinear spectral carriers for optical communication systems employing the nonlinear Fourier transform," *IEEE Commun. Lett.*, vol. 26, no. 1, pp. 109–112, Jan. 2022.
[11] M. Balogun and S. Derevyanko, "Enhancing the spectral efficiency of nonlinear frequency division multiplexing systems via Hermite-Gaussian subcarriers," *J. Lightw. Technol.*, vol. 40, no. 18, pp. 6071–6077, Sep. 15, 2022.

[12] T. Moazzeni, "On the compactness of OFDM and Hermite signals," *IEEE Commun. Lett.*, vol. 20, no. 7, pp. 1313–1316, Jul. 2016.
[13] M. Pankratova, A. Vasylchenkova, S. A. Derevyanko, N. B. Chichkov, and J. E. Prilepsky, "Signal-noise interaction in optical-fiber communication systems employing nonlinear frequency-division multiplexing," *Phys. Rev. Appl.*, vol. 13, no. 5, May 2020, Art. no. 054021.
[14] Q. Zhang and F. R. Kschischang, "Correlation-aided nonlinear spectrum detection," *J. Lightw. Technol.*, vol. 39, no. 15, pp. 4923–4931, Aug. 2021.
[15] M. Balogun, S. Derevyanko, and L. Barry, "Dual-polarization Hermite-Gaussian NFDM transmission with a single parameter equalizer," in *Proc. Conf. Lasers Electro-Opt. (CLEO)*, San Jose, CA, USA, 2023, pp. 1–2.
[16] R. J. Essiambre, R. Tkach, and R. Ryf, "Fiber nonlinearity and capacity: Single mode and multimode fibers," in *Optical Fiber Telecommunications VB: Systems and Networks*, I. Kaminow, T. Li, and A. Willner, Eds. Cambridge, MA, USA: Academic Press, 2013.
[17] S. T. Le, J. E. Prilepsky, and S. K. Turitsyn, "Nonlinear inverse synthesis technique for optical links with lumped amplification," *Opt. Exp.*, vol. 23, no. 7, pp. 8317–8328, 2015.
[18] X. Yangzhang, V. Aref, S. T. Le, H. Buelow, D. Lavery, and P. Bayvel, "Dual-polarization non-linear frequency-division multiplexed transmission with *b*-modulation," *J. Lightw. Technol.*, vol. 37, no. 6, pp. 1570–1578, Mar. 15, 2019.
[19] S. A. Derevyanko, M. Balogun, O. Aluf, D. Shepelsky, and J. Prilespky, "Channel model and the achievable information rates of the optical nonlinear frequency division-multiplexed systems employing continuous b-modulation," *Opt. Exp.*, vol. 29, no. 5, pp. 6384–6406, 2021.
[20] J.-W. Goossens, M. I. Yousefi, Y. Jaouán, and H. Hafermann, "Polarization-division multiplexing based on the nonlinear Fourier transform," *Opt. Exp.*, vol. 25, no. 22, pp. 26437–26452, Oct. 2017.
[21] S. Chimmalgi and S. Wahls, "Bounds on the transmit power of b-modulated NFDM systems in anomalous dispersion fiber," *Entropy*, vol. 22, no. 6, p. 639, Jun. 2020.
[22] D. M. Arnold, H.-A. Loeliger, P. O. Vontobel, A. Kavcic, and W. Zeng, "Simulation-based computation of information rates for channels with memory," *IEEE Trans. Inf. Theory*, vol. 52, no. 8, pp. 3498–3508, Aug. 2006.
[23] S. A. Derevyanko, J. E. Prilepsky, and S. K. Turitsyn, "Capacity estimates for optical transmission based on the nonlinear Fourier transform," *Nature Commun.*, vol. 7, no. 1, p. 307, Sep. 2016.

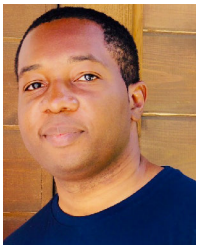

MUYIWA BALOGUN received the Ph.D. degree in electrical and information engineering from the University of the Witwatersrand, Johannesburg, South Africa, in 2018.

From 2018 to 2020, he was a Postdoctoral Research Fellow with the Center for Telecommunications and Access and Services, University of the Witwatersrand, and from 2020 to 2022, he was a Research Fellow with the Ben-Gurion University of the Negev, Israel. Currently, he is an IPIC Researcher with the Radio and Optical Communications Laboratory, School of Electronic Engineering, Dublin City University, within the Marie Sklodowska-Curie Actions (MSCA)/Science Foundation Ireland (SFI) SPARKLE Project. His current research interests include high-capacity optical communication systems, digital signal processing, and algorithm development.

STANISLAV DEREVYANKO received the Ph.D. degree in theoretical physics from the Institute for Radio Physics and Electronics, Kharkiv, Ukraine, in 2001.

From 2002 to 2007, he was twice a Postdoctoral Research Fellow with the Photonics Research Group, Aston University, Birmingham, U.K., and from 2007 to 2012, he was an EPSRC Advanced Fellow with the Nonlinearity and Complexity Research Group, Aston University. From 2013 to 2015, he was a Marie Curie Visiting Fellow with the Weizmann Institute of Science, Israel. In 2015, he joined the Department of Electrical and Computer Engineering, Ben-Gurion University of the Negev, Beersheba, Israel. His research interests include nonlinear optics, optical telecommunications, and information theory.

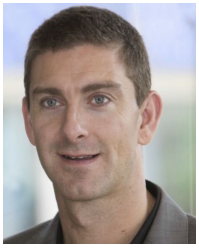

LIAM BARRY (Senior Member, IEEE) received the B.E. degree in electronic engineering and the M.Eng.Sc. degree in optical communications from University College Dublin, in 1991 and 1993, respectively, and the Ph.D. degree from the University of Rennes, France, for his work on all-optical switching technologies.

From February 1993 to January 1996, he was a Research Engineer with the Optical Systems Department, France Telecom's Research Laboratories (now known as Orange Labs), Lannion, France. In February 1996, he joined the Applied Optics Centre, Auckland University, New Zealand, as a Research Fellow, before taking up a lecturing position with the School of Electronic Engineering, Dublin City University, and establishing the Radio and Optical Communications Laboratory, in 1998. He is currently a Full Professor with the School of Electronic Engineering and a Principal Investigator for Science Foundation Ireland. His main research interests include all-optical signal processing and characterization, hybrid radio/fiber communication systems, wavelength tunable lasers, and optical frequency combs for high capacity systems. He has published over 600 papers in internationally peer reviewed journals and conferences, holds nine patents in the area of optoelectronics and has supervised 40 research graduate students to completion, with 32 at Ph.D. level. He has been a TPC Member for the European Conference on Optical Communications (ECOC) and the Optical Fiber Communication Conference (OFC), and served as the Chair for ECOC, in 2019. He became a member of the Royal Irish Academy, in 2019, and he was appointed to the Board of the Irish Research Council by the Minister of Education, in 2019.